ISSN 2616-5767 Vol.9, Issue 2: 95-102, DOI: 10.25236/AJETS.2026.090213

Layout-Aware Path Planning for Substation Inspection Robots Using Enhanced RRT*

Shihan Fang

University of Shanghai for Science and Technology, Shanghai, 200093, China

Abstract: *Path planning for substation inspection robots faces significant challenges in environments characterized by densely distributed equipment and narrow passages, which severely degrade the sampling efficiency and convergence speed of conventional algorithms. To address these limitations, this paper proposes an enhanced Rapidly-exploring Random Tree* (RRT*) framework that explicitly exploits the structured spatial layout of substations. Specifically, the proposed approach overcomes existing bottlenecks by introducing a Dynamic Constrained Sampling Space (DCSS) model to restrict exploration within task-relevant regions and minimize invalid samples; implementing a spatial adaptive adjustment strategy to dynamically guide tree expansion around large-scale equipment and prevent local stagnation; and integrating a multi-level dynamic rewiring mechanism to eliminate redundant intermediate nodes and enhance path structural continuity. Comprehensive simulations conducted in representative layout scenarios demonstrate the superiority of the proposed framework. The results indicate that this method provides a highly efficient and reliable navigation solution for intelligent substation inspection.*

Keywords: *Navigation, Mobile robot motion-planning, Substations, Algorithms*

1. Introduction

Autonomous robotic inspection is essential for modern substations, heavily relying on efficient path planning. However, substation environments pose unique geometric challenges: the standardized, grid-like layouts consist of diverse equipment—from massive transformers to dense lightning arresters—creating complex, narrow passages [1]-[4]. While traditional grid-based (e.g., A*) and bio-inspired (e.g., ACO) methods [5]-[7] suffer from discretization limits or unpredictable convergence in such constrained spaces, the Rapidly-exploring Random Tree* (RRT*) algorithm offers a promising continuous-space alternative.

Despite its asymptotic optimality, directly applying conventional RRT* to substations reveals two critical limitations: (1) its undirected uniform sampling generates massive invalid nodes within densely packed obstacle regions, severely degrading search efficiency [8]; and (2) its standard expansion and rewiring mechanisms fail to exploit the geometric regularity of equipment, leading to excessive redundant nodes, jagged detours, and local stagnation in narrow corridors.

To overcome these bottlenecks, this paper proposes an enhanced, layout-aware RRT* framework that explicitly embeds the structural characteristics of substations into the planning process. The main contributions are twofold:

Layout-Aware Sampling and Adaptive Expansion: We introduce a Dynamic Constrained Sampling Space (DCSS) to restrict exploration within task-relevant regions, fundamentally reducing invalid samples. Concurrently, a spatial adaptive adjustment strategy is proposed to intelligently guide tree expansion around varying-sized obstacles, effectively preventing local blockages.

Multi-Level Dynamic Rewiring: To eliminate the jagged paths typical of sampling-based planners, a structured parent node backtracking and reconnection mechanism is developed. This strategy significantly reduces unnecessary direction changes and improves trajectory continuity.

Extensive simulations in representative substation layouts (simple, complex, and narrow passages) demonstrate that the proposed method significantly outperforms conventional planners, achieving faster convergence and shorter, smoother paths.

ISSN 2616-5767 Vol.9, Issue 2: 95-102, DOI: 10.25236/AJETS.2026.090213

2. Related works

Path planning algorithms for mobile robots can be broadly categorized into grid-based, bio-inspired, and sampling-based approaches. While each has been applied to robotic navigation, their performance in highly constrained and structured environments like substations varies significantly.

Grid-based and Bio-inspired Methods: Grid-based algorithms, predominantly A* and Dijkstra's, are widely used due to their determinism. Recent improvements have focused on heuristic function design [9], [10] and multi-directional search [11] to improve path smoothness. However, their reliance on explicit environmental discretization inherently restricts their scalability in large-scale continuous spaces, leading to massive memory overhead in complex substations. Alternatively, bio-inspired algorithms like Ant Colony Optimization (ACO) [12], [13] offer global search capabilities. Various hybridizations, such as combining ACO with artificial potential fields [14], have been proposed to accelerate convergence. Despite these enhancements, bio-inspired methods, including Particle Swarm Optimization (PSO) [15], frequently suffer from parameter sensitivity and unpredictable convergence behavior, easily falling into local optima when navigating the dense, maze-like layouts of substations.

Sampling-based Methods: Operating directly in continuous space, the Rapidly-exploring Random Tree* (RRT*) algorithm ensures asymptotic optimality without discretization [8]. However, the uniform sampling nature of basic RRT* yields low efficiency in environments with dense obstacles. To mitigate this, Fast-RRT* [16] and MQ-RRT* [17] introduced goal-biased and sparse optimized sampling to accelerate convergence. While these RRT* variants improve general planning efficiency, they treat all obstacles uniformly. They fail to exploit the inherent geometric regularities (e.g., grid-like arrangements) and extreme scale variations (e.g., large transformers vs. small sensors) present in substations. Consequently, these methods still generate excessive invalid samples and struggle to efficiently traverse narrow inter-equipment passages, a gap this paper aims to bridge by integrating layout-aware spatial constraints.

3. The Proposed RRT* Algorithm

3.1. Dynamic Constrained Sampling Space

Substation environments inherently feature highly regular, grid-like equipment layouts mandated by standardized industry designs. However, conventional RRT* relies on a global uniform sampling strategy that completely ignores this structural prior. Consequently, a massive number of random samples fall inside dense equipment regions, leading to severe computational waste, invalid node generation, and sluggish convergence. To overcome this inefficiency, we propose a Dynamic Constrained Sampling Space (DCSS) model that explicitly embeds the geometric characteristics of substations into the sampling process. Instead of sampling over the entire free space, DCSS restricts exploration to a dynamically adjusted rectangular area, mathematically defined as follows:

$$\mathcal{S}_{\text{sample}}^{(t)} = \left\{ \begin{array}{l} (x,y) \in \mathbb{R}^2 \mid \\ x_{\min}^{(t)} \le x \le x_{\max}^{(t)}, y_{\min}^{(t)} \le y \le y_{\max}^{(t)} \end{array} \right\} \tag{1}$$

Where x and y denote the planar coordinates of a sampling point; $x_{\min}^{(t)}$ and $x_{\max}^{(t)}$ represent the minimum and maximum sampling boundaries along the x-axis at time t, determined by the positions of the current node and the target point; $y_{\min}^{(t)}$ and $y_{\max}^{(t)}$ are the corresponding boundaries along the y-axis. These boundary parameters are dynamically updated according to:

$$\begin{cases} x_{\min}^{(t)} = \min\left(p_{\text{current}}^{(t)}(x), p_{\text{goal}}(x) \right) \\ x_{\max}^{(t)} = \max\left(p_{\text{current}}^{(t)}(x), p_{\text{goal}}(x) \right) \\ y_{\min}^{(t)} = \min\left(p_{\text{current}}^{(t)}(y), p_{\text{goal}}(y) \right) \\ y_{\max}^{(t)} = \max\left(p_{\text{current}}^{(t)}(y), p_{\text{goal}}(y) \right) \end{cases} \tag{2}$$

Where $p_{\text{current}}^{(t)}$ denotes the position of the current node at time t, and p_{goal} represents the target point. By constraining the sampling space to a dynamically evolving rectangular region defined by the current

ISSN 2616-5767 Vol.9, Issue 2: 95-102, DOI: 10.25236/AJETS.2026.090213

node and the goal, the DCSS model effectively leverages the inherent geometric regularity of substation environments. As the tree expands, the sampling boundaries are continuously refined, which substantially reduces the likelihood of invalid sampling and significantly improves the efficiency of the path search process.

3.2. Dynamic Spatial Adaptive Adjustment Strategy

While the Dynamic Constrained Sampling Space (DCSS) model significantly improves global sampling efficiency by exploiting the regular layout of substation environments, local planning bottlenecks may still arise when the dynamically defined sampling region is heavily affected by equipment geometry. In particular, the large variation in equipment size and spatial distribution within substations introduces additional challenges under the DCSS framework. Substation equipment can generally be classified into two categories: (1) large-scale equipment, such as main transformers and GIS combiners, whose monolithic structures occupy substantial regions of the workspace; and (2) small-scale equipment, including lightning arresters and terminal boxes, which are individually compact but densely distributed.

Under the DCSS framework, the sampling region is dynamically defined by the current node and the target point. When this rectangular region is partially or extensively intersected by equipment, the effective free space available for sampling may be severely reduced or fragmented, leading to a sharp decline in valid sample generation or repeated expansions around obstacle boundaries. These effects give rise to distinct local planning bottlenecks that cannot be resolved by DCSS alone.

To address the above problems, this paper proposes a dynamic adjustment strategy based on real-time spatial interference analysis, incorporating the size distribution characteristics of substation equipment. This strategy first detects two types of interference states online: Type I parallel interference (large-volume penetration), triggered when two parallel sides of the sampling rectangle simultaneously intersect with the boundary of a single large-scale equipment (e.g., traversing the long side of a main transformer); Type II vertical interference (small-volume circumvention), triggered when two perpendicular sides of the sampling rectangle simultaneously intersect with multiple small-scale equipment (e.g., traversing an array of lightning arresters). Based on the detected interference state, the system executes three adjustment strategies to calculate the optimal boundary obstacle vertex, thereby guiding new sampling points to overcome obstacles quickly:

1) If only Type I interference exists, adjust according to (3):

$$\mathbf{v}_{\text{nearest1}} = \arg\min_{\mathbf{v}\in\mathcal{V}_O} \| p_{\text{current}} - \mathbf{v} \|_2 \tag{3}$$

2) If only Type II interference exists, adjust according to (4):

$$\mathbf{v}_{\text{nearest2}} = \arg\min_{\mathbf{v}\in\mathcal{V}_O} \| p_{\text{valid}} - \mathbf{v} \|_2 \tag{4}$$

3) If both Type I and Type II interference exist, adjust according to (5):

$$\begin{cases} \mathbf{v}_{\text{nearest1}} = \arg\min_{\mathbf{v}\in\mathcal{V}_O} \| p_{\text{current}} - \mathbf{v} \|_2 \\ \mathbf{v}_{\text{nearest2}} = \arg\min_{\mathbf{v}\in\mathcal{V}_O} \| p_{\text{valid}} - \mathbf{v} \|_2 \end{cases} \tag{5}$$

Where $\mathbf{v}_{\text{nearest1}}$ is the nearest vertex coordinate of the obstacle in Type I interference, $\mathbf{v}_{\text{nearest2}}$ is the nearest vertex coordinate of the obstacle in Type II interference, $\mathcal{V}_O$ represents the vertex set of the obstacle, p_{current} is the current point coordinate, and p_{valid} is a feasible point generated through p_{current} and p_{goal}, defined by the following (6):

$$p_{\text{valid}} \in \left\{ \begin{bmatrix} p_{\text{current}}^{(x)} \\ p_{\text{goal}}^{(y)} \end{bmatrix}, \begin{bmatrix} p_{\text{goal}}^{(x)} \\ p_{\text{current}}^{(y)} \end{bmatrix} \right\} \tag{6}$$

Furthermore, it satisfies $p_{\text{valid}} \notin \bigcup_i \text{Obstacle}_i$, meaning this valid point is not located inside any obstacle.

The reconstruction of the sampling space is handled separately based on the interference type: If only a single interference exists, traverse all vertices of the corresponding obstacle, select the vertex with the

ISSN 2616-5767 Vol.9, Issue 2: 95-102, DOI: 10.25236/AJETS.2026.090213

shortest Euclidean distance to the current point p_{current} or the feasible point p_{valid}, and use it as the target positioning point for the new sampling space. If both types of interference occur, calculate $\mathbf{v}_{\text{nearest1}}$ and $\mathbf{v}_{\text{nearest2}}$ separately, and according to the relative orientation between obstacles and the current node position, select the final vertex based on the following rules:

If the Type I obstacle is located to the left/right of the Type II obstacle:

1) When the current point p_{current} is located to the left/right of the Type I obstacle, select $\mathbf{v}_{\text{nearest1}}$.

2) When the current point p_{current} is located to the top/bottom of the Type II obstacle, select $\mathbf{v}_{\text{nearest2}}$.

If the Type I obstacle is located to the top/bottom of the Type II obstacle:

1) When the current point p_{current} is located to the top/bottom of the Type I obstacle, select $\mathbf{v}_{\text{nearest1}}$.

2) When the current point p_{current} is located to the left/right of the Type II obstacle, select $\mathbf{v}_{\text{nearest2}}$.

Subsequently, expand the sampling area boundary along the obstacle's normal direction. The following formula determines the expansion magnitude Δd:

$$\begin{cases} \Delta d1 = \| p_{\text{current}} - \mathbf{v}_{\text{nearest1}} \|_2 \\ \Delta d2 = \| p_{\text{current}} - \mathbf{v}_{\text{nearest2}} \|_2 \end{cases} \tag{7}$$

In addition to expanding the boundary in a single direction (longitudinal or transverse), a fixed step size δ is introduced to compensate for the vertical direction, effectively avoiding falling into local optima.

For the single interference scenario, differentiated expansion strategies are formulated based on the current point's orientation relative to the obstacles (left, right, top, bottom):

Scheme 1: When located to the left or right of all obstacles, perform horizontal expansion:

$$\begin{cases} y_{\max} \leftarrow y_{\max} + \Delta d \\ y_{\min} \leftarrow y_{\min} - \Delta d \\ x_{\min} \leftarrow x_{\min} - \delta_{\text{left}} \,\|\, x_{\max} \leftarrow x_{\max} + \delta_{\text{right}} \end{cases} \tag{8}$$

Scheme 2: When located to the top or bottom of all obstacles, perform vertical expansion:

$$\begin{cases} x_{\max} \leftarrow x_{\max} + \Delta d \\ x_{\min} \leftarrow x_{\min} - \Delta d \\ y_{\max} \leftarrow y_{\max} + \delta_{\text{above}} \,\|\, y_{\min} \leftarrow y_{\min} - \delta_{\text{below}} \end{cases} \tag{9}$$

For the mixed interference scenario (assuming Type I corresponds to obstacle 1, Type II corresponds to obstacle 2), execute based on the relative position of obstacles and the current point's orientation:

Scheme 3:

1) If obstacle 1 is located to the left/right of obstacle 2, and the current point is located to the left/right of obstacle 2, adjust according to:

$$\begin{cases} y_{\max} \leftarrow y_{\max} + \Delta d1 \\ y_{\min} \leftarrow y_{\min} - \Delta d1 \\ x_{\min} \leftarrow x_{\min} - \delta_{\text{left}} \,\|\, x_{\max} \leftarrow x_{\max} + \delta_{\text{right}} \end{cases} \tag{10}$$

2) If obstacle 1 is located to the left/right of obstacle 2, and the current point is located to the top/bottom of obstacle 2, adjust according to:

$$\begin{cases} x_{\max} \leftarrow x_{\max} + \Delta d2 \\ x_{\min} \leftarrow x_{\min} - \Delta d2 \\ y_{\max} \leftarrow y_{\max} + \delta_{\text{above}} \,\|\, y_{\min} \leftarrow y_{\min} - \delta_{\text{below}} \end{cases} \tag{11}$$

Scheme 4:

1) If obstacle 1 is located to the top/bottom of obstacle 2, and the current point is located to the top/bottom of obstacle 2, adjust according to:

ISSN 2616-5767 Vol.9, Issue 2: 95-102, DOI: 10.25236/AJETS.2026.090213

$$\begin{cases} x_{\max} \leftarrow x_{\max} + \Delta d1 \\ x_{\min} \leftarrow x_{\min} - \Delta d1 \\ y_{\max} \leftarrow y_{\max} + \delta_{\text{above}} \,||\, y_{\min} \leftarrow y_{\min} - \delta_{\text{below}} \end{cases} \tag{12}$$

2) If obstacle 1 is located to the top/bottom of obstacle 2, and the current point is located to the left/right of obstacle 2, adjust according to:

$$\begin{cases} y_{\max} \leftarrow y_{\max} + \Delta d2 \\ y_{\min} \leftarrow y_{\min} - \Delta d2 \\ x_{\min} \leftarrow x_{\min} - \delta_{\text{left}} \,||\, x_{\max} \leftarrow x_{\max} + \delta_{\text{right}} \end{cases} \tag{13}$$

By incorporating prior knowledge of equipment sizes, the strategy enables the sampling space to continually expand directionally around the optimal vertex, significantly enhancing the algorithm's efficiency in bypassing obstacles while ensuring the quality of the path.

3.3. Dynamic Rewiring Strategy

While the dynamic sampling and spatial adaptive adjustment strategies described in Section III-B and Section III-C effectively guarantee path feasibility in complex substation environments, the initially generated paths may still exhibit suboptimal structural quality.

To address these issues, this paper proposes a dynamic rewiring strategy that focuses on optimizing path continuity and length through structured parent node reconstruction under strict safety constraints. Rather than explicitly modeling curvature or higher-order smoothness metrics, the proposed strategy improves motion continuity by reducing redundant nodes and unnecessary direction changes through multi-level parent backtracking and reconnection. The strategy adopts a three-stage progressive optimization framework, described as follows.

First, a benchmark cost evaluation model is established. The cumulative path cost from the start node to a newly generated node is computed by recursively backtracking along the parent node chain. The Euclidean distance of each local segment is used as the cost metric, and the global cost is obtained through reverse traversal of the tree structure. This process provides a stable reference baseline for evaluating alternative parent connections during subsequent optimization.

Second, a feasibility-oriented neighborhood screening mechanism is applied. Within a dynamically defined neighborhood radius, a candidate parent node set is constructed. Each candidate node is filtered using a dual-constraint condition. The first constraint enforces safety and feasibility by performing collision detection on the straight-line segment connecting the candidate node and the new node, ensuring that the path segment does not intersect any obstacle. The second constraint restricts spatial proximity, limiting candidate nodes to a local neighborhood in order to maintain computational efficiency and prevent excessive rewiring.

Finally, a cost-driven dynamic parent reselection process is executed. For each candidate node that satisfies the feasibility constraints, the corresponding global path cost is recalculated assuming it is selected as the new parent. By comparing this cost with the benchmark cost, the algorithm dynamically selects the parent node that minimizes the overall path length. This multi-level backtracking and reconnection process significantly reduces redundant intermediate nodes and eliminates unnecessary detours, resulting in paths with fewer discrete turning points and improved structural continuity.

4. Simulation Analysis Based on MATLAB

4.1. Experimental Environment Configuration

To systematically validate the performance of the improved RRT* algorithm under different environmental conditions, comparative experiments are conducted in three representative substation scenarios. As shown in Figure 1, the simulation environments include three types: (a) simple environment; (b) complex environment; (c) narrow passage environment. The enormous rectangular obstacles in the environment simulate large-scale equipment such as main transformers and GIS combiners, while the small rectangular obstacles simulate smaller-scale equipment, including lightning arresters and terminal boxes. Both simple and complex environments are composed of the aforementioned two types of obstacles at different densities.

ISSN 2616-5767 Vol.9, Issue 2: 95-102, DOI: 10.25236/AJETS.2026.090213

In contrast, the narrow passage environment is used to simulate scenarios with sudden channel narrowing caused by cable layers, gaps in distribution rooms, or maintenance safety fences, testing the algorithm's extreme passing capability.

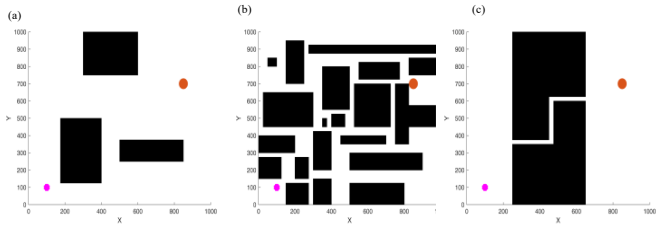

Figure 1: simulation environments.

The hardware platform configuration for running the experiments consisted of an Intel Core i5-9300H processor at 2.40 GHz, a 500 GB solid-state drive, and 8 GB of RAM. The software environment consisted of the MATLAB simulation platform running on the Windows 10 operating system. All simulation experiments were conducted under the same map size (1000 × 1000 pixels). The start and end points were set at diagonal positions on the map, with the start point coordinate at (100, 100) and the end point coordinate at (850, 700). The maximum number of iterations for the algorithm was uniformly set to 20,000, and the step size was set to 15.

4.2. Experimental Results and Analysis

To comprehensively evaluate the performance of the improved RRT* algorithm (Opt-RRT*), this paper compares it with five mainstream path planning algorithms: RRT*[8], A*[5], RRT-connect [18], Fast-RRT*[16], MQ-RRT*[17]. The visual comparison results of the path planning for the six algorithms in the three environments are shown in Figures 2–4. For clarity, the visual elements in these figures are described as follows: the pink and orange dots denote the start and goal points, respectively. Yellow lines represent redundant exploration branches generated during random sampling, green lines indicate exploration paths expanded from the goal direction, cyan lines correspond to locally optimized paths during the planning process, and blue lines depict the final planned paths obtained after optimization.

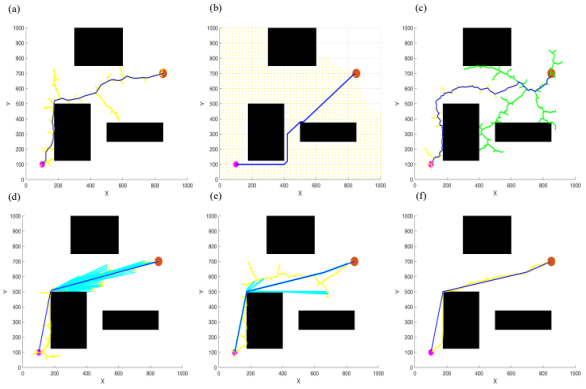

Figure 2: Experimental Results in a Simple Environment.

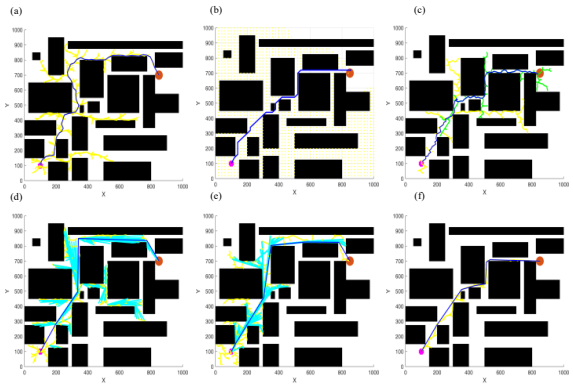

Figure 3: Experimental Results in Complex Environments.

ISSN 2616-5767 Vol.9, Issue 2: 95-102, DOI: 10.25236/AJETS.2026.090213

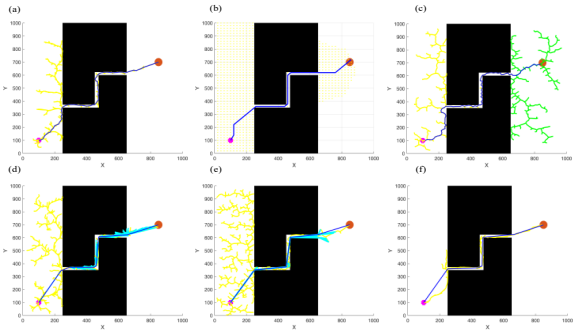

Figure 4: Experimental Results in a Narrow Channel Environment.

From visual inspection of Figures 2-4, the proposed Opt-RRT* algorithm exhibits several consistent advantages across different environments. Compared with the other methods, its generated random trees are noticeably sparser, with fewer redundant exploration branches, indicating effective suppression of invalid sampling. The resulting planned paths are more direct, showing fewer unnecessary detours and turning points, especially in structured corridors. Moreover, in narrow passage scenarios, Opt-RRT* demonstrates stronger spatial focus, with exploration and optimization processes concentrated around the feasible channel, enabling stable and accurate traversal through constrained regions.

5. Conclusion

This paper investigates the path planning problem of substation inspection robots operating in environments characterized by dense equipment layouts and narrow passages, where conventional sampling-based planners struggle with low efficiency and high path redundancy. To address these challenges, a layout-aware global path planning framework based on an enhanced RRT* algorithm is proposed. By explicitly incorporating the structured spatial layout of substations and equipment scale diversity, the proposed method introduces a Dynamic Constrained Sampling Space (DCSS), spatial adaptive adjustment mechanisms, and a multi-level dynamic rewiring strategy. These designs enable the planner to fundamentally reduce invalid sampling, prevent local stagnation, and generate smooth paths in complex environments. Extensive simulation experiments in representative substation scenarios validate the effectiveness of the proposed approach. The results demonstrate that the improved RRT* algorithm achieves superior performance in convergence speed, path continuity, and node efficiency compared with conventional methods, with particularly pronounced advantages in highly constrained narrow passages. Future work will focus on deploying the proposed framework on physical inspection robots and extending it to dynamic environments with moving obstacles

References

[1] T. Zhang, and J. Dai, "Electric power intelligent inspection robot: a review." J. Phys.: Conf. Ser., 2021, Art. no. 012023.
[2] S. Lu, Y. Zhang, and J. Su, "Mobile robot for power substation inspection: A survey," IEEE/CAA Journal of Automatica Sinica, vol. 4, no. 4, pp. 830-847, Oct. 2017.
[3] H. Ye, H. Tian, Q. Wu, Y. Xue, J. Xiao, G. Liu, and Y. Xiong, "Synergistic Hierarchical AI Framework for USV Navigation: Closing the Loop Between Swin-Transformer Perception, T-ASTAR Planning, and Energy-Aware TD3 Control," Sensors, vol. 25, no. 15, pp. 4699, Aug. 2025.
[4] Z. Liu, A. Pan, A. Jiang, W. Li, J. Zhang, and C. Bai, "Research on Decoupling Motion Path Planning of Two Manipulators of Live Working Robot Based on Hybrid RRT Algorithm." in Proc. 4th World Conf. Mech. Eng. Intell. Manuf. (WCMEIM), 2021, pp. 278–282.
[5] P. E. Hart, N. J. Nilsson, and B. Raphael, "A formal basis for the heuristic determination of minimum cost paths," IEEE Trans. Syst. Sci. Cybern., vol. 4, no. 2, pp. 100-107, July 1968.
[6] M. Dorigo, V. Maniezzo, and A. Colorni, "Ant system: optimization by a colony of cooperating agents," IEEE Trans. Syst., Man, Cybern. B, vol. 26, no. 1, pp. 29-41, Feb. 1996.
[7] J. Kennedy, and R. Eberhart, "Particle swarm optimization," in Proc. IEEE Int. Conf. Neural Netw., Perth, WA, Australia, 1995, pp. 1942-1948.
[8] S. Karaman and E. Frazzoli, "Sampling-based algorithms for optimal motion planning," Int. J. Robot. Res., vol. 30, no. 7, pp. 846–894, June 2011.
[9] P. Luo, B. Li, X. Xue, and Z. Liu, "Research on path planning of substation inspection robot based

ISSN 2616-5767 Vol.9, Issue 2: 95-102, DOI: 10.25236/AJETS.2026.090213

on improved A algorithm," in Proc. China Autom. Congr. (CAC), Xiamen, China, 2022, pp. 1119–1124.*
[10] C. Mao, J. Ma, P. Qi, and D. Wang, "Novel path planning algorithm for the mobile robot in power transformer substation," Int. Trans. Electr. Energy Syst., vol. 2025, no. 1, 2025.
[11] J. Huang, C. Chen, J. Shen, G. Liu, et al., "A self-adaptive neighborhood search A-star algorithm for mobile robots global path planning," Comput. Electr. Eng., vol. 123, 2025.
[12] G. Li, C. Liu, L. Wu, and W. Xiao, "A mixing algorithm of ACO and ABC for solving path planning of mobile robot," Appl. Soft Comput., vol. 148, Art. no. 110868, Dec. 2023.
[13] Y. Xu, Q. Jin, and Y. Zhang, "A path planning method for mobile robots incorporating artificial potential field method and ant colony algorithm," in Proc. Int. Conf. Autom. Control, Algorithm, Intell. Bionics (ACAIB), 2023, pp. 346–353.
[14] W. Wang, X. Yin, S. Wang, J. Wang, et al., "Robot path planning method combining enhanced APF and improved ACO algorithm for power emergency maintenance," Int. J. Inf. Technol. Syst. Approach, vol. 16, no. 3, 2023.
[15] Q. Su and Y. Cai, "Path planning for power inspection robot based on improved PSO algorithm and dynamic window approach," in Proc. 5th Int. Conf. Inf. Sci., Parallel Distrib. Syst. (ISPDS), Guangzhou, China, 2024, pp. 498–502.
[16] Q. Li, J. Wang, H. Li, B. Wang, and C. Feng, "Fast-RRT: An improved motion planner for mobile robot in two-dimensional space," IEEJ Trans. Electr. Electron. Eng., vol. 16, no. 10, pp. 1451–1460, Oct. 2021.*
[17] X. Cui et al., "More quickly-RRT: Improved quick rapidly-exploring random tree star algorithm," Eng. Appl. Artif. Intell., vol. 133, Art. no. 108246, July 2024.*
[18] J. J. Kuffner and S. M. LaValle, "RRT-connect: An efficient approach to single-query path planning," in Proc. IEEE Int. Conf. Robot. Autom. (ICRA), San Francisco, CA, USA, vol. 2, Apr. 2000, pp. 995–1001.